International Journal of Engineering Research and Reviews ISSN 2348-697X (Online)
Vol. 5, Issue 2, pp: (21-29), Month: April - June 2017, Available at: www.researchpublish.com

Circuit Designing of Bio-Magnetic Sensor Using Giant Magneto-Impedance Effect

Mrs. Nilima A. Warade

Department of Humanities Vidya Prasarak Mandal's Polytechnic Thane, India, 400601

***Abstract*: The detection of bio-magnetic activities enables non-contact and non-invasive evaluation of electrical activity in living organisms. In this paper a practical method to achieve bio-magnetic field detection in non-magnetically shielded environment at the RT in introduced. This method is based on Giant Magneto-Impedance (GMI) Effect in amorphous wire. At first, bio-magnetic fields and the principal of GMI effect are reviewed. After that off-diagonal GMI effect measurement experiment is carried out to obtain the circuit design requirement. The experimental result is formed that, if the sensitivity of GMI sensors reach to 10 pico-Tesla (pT) level, the gain of amplifier circuit should be more than 10 thousand times. It is almost impossible to obtain so much gain by only one order amplifier circuit, so the circuit was designed using several orders for sake of a stable and high gain (A>=100,000). Usually in non-magnetically shielded environment, the fluctuation of power frequency interference is about nanoTesla (nT) level. Hence, some notch filter circuits were designed to eliminate power frequency interference and to prevent circuit saturation. As the bio-magnetic fields distribute in the low frequency domain, we filtered out the frequency above 200 Hz. In the last part performance testing is carried out. We utilized a long enough straight wire to generate weak magnetic field for sensitivity testing, we could infer that the bio-sensor sensitivity is near to 10pT in non-magnetically shielded environment.**

***Keywords:* Amorphous wire, Bio-magnetic field, GMI sensor, Pico-Tesla bio-magnetic sensor.**

I. INTRODUCTION

Bio-magnetic refers to the study of the body`s own magnetic field. These fields are extremely week and are only detectable with exquisitely sensitive equipment that blocks out all external magnetic fields, including the Earth`s magnetic field. Conventionally, these bio-magnetic signals are detected by superconducting quantum interference device (SQUID) in magnetically shielded room(MSR), with sensitivity at the femto-Tesla (fT) level. However, this technology requires special equipment, such as container of cooling liquid medium and a magnetic shield room. Therefore, the SQUID system is too large and expensive for personal and single laboratory use [4, 5].

In general, the human magnetic fields are at pT level. So, we need extreme sensitive micro-magnetic sensor to detect bio-magnetic fields. In 1993, Professor K. Mohri found a new electromagnetic phenomenon in the amorphous wire and named it as GMI effect, in which the impedance of the amorphous wire sensitively changed with a small external applied magnetic field when a high-frequency current was applied through the wire as a carrier [3]. Based on GMI effect, they have developed sensitive micro magnetic sensors, called" MI sensor", with the sensitivity of 1pT level (Uchiyama et al, 2009), and they have realized bio-magnetic field detecting in non-magnetically shielded environment at the room temperature.

From TABLE I, the field detection resolution of the fluxgate sensor was about 1Oe for ac uniform fields and about 100Oe for a dc field, and the quick response frequency and power consumption, such as the Hall, MR, and GMR sensors, were about 1MHz and about 10mW, respectively [1-9]. In comparison with conventional magnetic sensors [Hall sensor, the magneto resistive (MR) sensor, the giant magneto resistive (GMR) sensor] the MI sensor has the advantageous feature of high sensitivity. Fig. 1 illustrates the configuration of the magnetic sensor utilizing amorphous wire.

TABLE I COMPARISON OF MAGNETIC SENSORS

Sensor	Head length (ɜm)	Resolution (10^{-4}T)	Response speed	Power consumption
Hall sensor	10~100	0.5/±1k*	1MHz	10mW
MR sensor	10~100	0.1/±100	1MHz	10mW
GMR sensor	10~100	0.01/±20	1MHz	10mW
Fluxgate	10~20	1ɜ/±3	5kHz	1W
MI sensor	1k~2k	1ɜ/±3	1Mhz	10mW

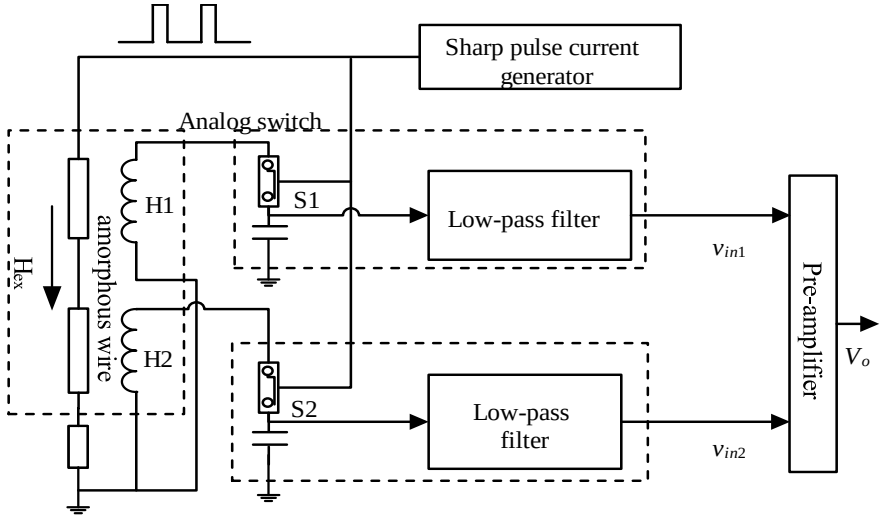

Fig. 1. The magnetic sensor circuit based on GMI effect using sharp pulse current to drive amorphous wire

II. BIO-MAGNETIC FIELDS

TABLE II shows the comparison between some common magnetic fields, which were generated by different parts of the human body. It can be easily concluded that the human bio-magnetic field is extremely weak, near 10^{-6} times as much as the geomagnetic field. Therein, the brain magnetic field is weakest among all human bio-magnetic fields. While the higher-intensity magnetic field is the heart magnetic field.

TABLE II THE HUMAN BIO-MAGNETIC FIELD INTENSITY

	Magnetic source	Magnetic intensity (10^{-4}T)
Inside magnetic	Lung	10^{-4}
	Belly	10^{-8}
	Heart	10^{-6}
	Brain-magnetic	10^{-8}
	Brain cortex	10^{-9}
Outside magnetic	Geomagnetic field	10^{-1}
	Magnetic storm fluctuation	10-5~10-3
	Urban electromagnetic noise	10^{-3}

Sources of electromagnetic radiations like power lines, microwave, telecommunication, electrical appliances, radar, transmission radio and television, etc. increasing rapidly. These are causing serious electromagnetic pollutions around our living environment. Common urban electromagnetic disturbance is more than 1,000 times versus the magnetic fields

among people. Therefore, the measurement of these bio-magnetic fields under non-MSR mean to extract extremely weak magnetic signal from a few ten thousand times of electromagnetic disturbance environment. Hence, those disturbances should be eliminated for bio-magnetic field detection in non-MSR.

The main frequency components of bio-magnetic is dispersed in low frequency domain, mainly below 500Hz.

For example, the magneto-encephalography (MEG), which can be utilized as brain-computer interface (BCI) input signal, ranges from 5Hz to 200Hz [4]. Wherein alpha waves are present in the occipital region of the brain while the subject's eyes are closed and disappear when the eyes opened, which is replaced by beta waves [17]. Alpha waves are present in the occipital region of the brain while the subject`s eyes are closed. These waves are disappeared when the eyes are open and replaced by beta waves. Alpha waves and beta waves range in frequency from 8Hz to 13Hz and 14Hz to 30Hz, respectively. So, in this article, the circuit is designed for bio-magnetic field detection should filter out high frequency components [12].

III. PRINCIPLE OF GMI EFFECT

When a soft ferromagnetic conductor is subjected to a small alternating current (ac), a large change in the ac complex impedance of the conductor can be achieved upon applying a magnetic field. This is known as the GMI effect. The GMI effect can be theoretical explained by skin effect in the amorphous wires [1-9]. The principal expression of the GMI effect in amorphous wires is as follows [2, 3]:

$$Z = (\frac{1}{2})\mathrm{R}_{dc}\, k\alpha \frac{J_0(\mathrm{k}\,\alpha)}{J_1(\mathrm{k}\,\alpha)},$$

$$k = \frac{1-j}{\delta}, \delta = \sqrt{\frac{2\rho}{w\mu}} \quad \text{(skin depth)} \qquad (1)$$

Where R_{dc} is the wire dc resistance, I is the wire radius, i is the skin depth, q is the resistivity, $\dot{A}$ is the angular frequency of the wire ac current, $\jmath$ is the circumferential maximum differential permeability, and J_0, J_1 are the Bessel functions of the 0-order and 1st-order.

When $\delta >> \alpha$ (no skin effect; $\omega << 2\rho/\mu\alpha^2$),

$$Z = R_{dc} + j\omega L,\ \mathrm{L} = \frac{\mu\ell}{8\pi} \qquad (2)$$

When $\delta << \alpha$ (strong skin effect; $\omega >> 2\rho/\mu\alpha^2$),

$$Z = \frac{(1+\mathrm{j})\alpha\,\mathrm{R}_{\mathrm{dc}}(\omega\mu(\mathrm{H}_{\mathrm{ex}}))^{\frac{1}{2}}}{2(2\rho)^{\frac{1}{2}}} \quad \text{(GMI effect)} \quad (3)$$

The magnitude of the wire impedance Z sensitively changes for an external magnetic field H_{ex} is expressed as:

$$\frac{\partial|Z|}{\partial Hex} = \frac{A\mu^{-\frac{1}{2}}\partial\mu}{\partial Hex},\quad \mathrm{A} = \frac{\rho^{\frac{1}{2}}\omega^{\frac{1}{2}}\ell}{4\pi\alpha} \qquad (4)$$

where ℓ the wire length. Per (2), (3) and (4), the permeability $\jmath$ depends on the driving frequency $\dot{A}$ and external magnetic field H_{ex}, namely $\jmath$ changes with $\dot{A}$ and H_{ex}. When the drive current frequency and amplitude of amorphous wire fixed, the impendence Z merely related to the change of external magnetic field H_{ex}. We can get the external magnetic changes by measuring the variety of amorphous wire impedance Z.

The GMI ratio, $\Delta Z/Z(\%)$, is defined as :

$$\Delta Z / Z(\%) = \frac{Z(\mathrm{H}) - Z(\mathrm{H}_{\max})}{Z(\mathrm{H}_{\max})} \times 100\% \qquad (5)$$

where H_{max} is, the external magnetic field leading to the maximum impedance [15]. In practice, the value of H_{max} depends on given experimental amorphous wire.

When the amorphous wires pass through the sharp pulse current, it also generates a strong skin effect, like the sinusoidal current. We can construct the GMI sensors based on sharp pulse GMI effect. For the purpose in this article, we simplify the transform, supposing that a sharp pulse current $i_p(t)$ with rising time t_r and magnitude I_p corresponds to a dc-biased sinusoidal current with a frequency f=1/2t_r as:

$$i_p(t) = (\frac{I_p}{2})(\frac{1+\sin \pi t}{t_r}) \quad (6)$$

Cite the Fig. 2 as example, the rising time is about 10 ns and corresponds to a sinusoidal current with around 50 MHz, which could induce a strong skin effect in the amorphous wire.

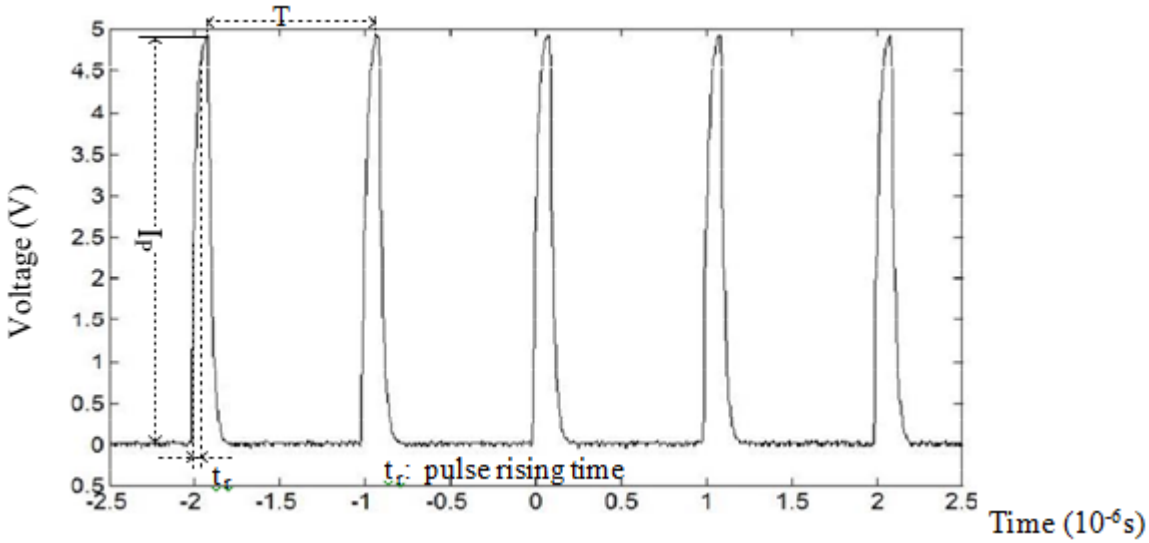

Fig. 2. The output waveform corresponds to 50MHz sinusoidal current.

The sharp pulse train current in practical engineering, with 10% duty cycle and 1 MHz frequency and is used for amorphous magnetization.

IV. CIRCUIT DESIGN REQUIREMENT

In Fig. 1 GMI gradiometer is constructed for the cancellation of background uniform noises, such as the geomagnetic field, to detect very weak magnetic field like bio-magnetic field. For this sensor head, the amorphous Co-Fe-Si-B wire (made by Ningbo Institute of Industrial Technology, CAS) has two coils: a sensing coil and a reference coil. The distance between the two pick up coils is set 3.5 cm. the sharp pulse current with 20% duty cycle and 2MHz frequency is subjected to amorphous wires. Meanwhile, a 500 turns induced coil, which is wound on the amorphous wire (50ȝm in diameter), is used to pick up the voltage reflecting external magnetic field variation.

Fig. 3 illustrates the circuit diagram for off-diagonal GMI effect measurement. The amorphous wire (50mm in diameter, 56mm in length), which is surrounded by a pickup coil (5mm in diameter, 100turns), is subjected to sharp pulse current (1MHz in frequency, 1.5V in amplitude (generated by DG4162, and corresponding current 1.5 mA). The external magnetic fields change from -0.3ȝT to 0.3ȝT along the same direction of amorphous wire. Fig.4 shows the induced voltage variation curves versus magnetic field changes. It is obvious that a weak hysteresis exists in amorphous wire, because the amorphous wire is too long.

In the off-diagonal GMI effect measurement experiment, when we utilized 100 turns pickup coil, the best linear region ranges from -0.02ȝT to 0.05ȝT, which is near 0.02ȝV/nT/turns (100V/T/turns). The induced voltage is proportion to the number of pickup coil [2]. Thus, if we use 500 turns pickup coil, the induction voltage will change about 10ȝV/nT. In addition, 5V sharp pulse current is applied to amorphous wire, instead of 1.5V. In this way, the induction voltage will change about 33ȝV/nT. If the biosensor conquers the resolution of 10 pico-Tesla (pT) level (0.033ȝV/pT) and we amplify

the induced voltage about 100 thousand times, the sensor output reaches to 3.3mV/pT. Because of length effect in amorphous, when we use 6mm amorphous wire to design sensor, the induced voltage will plunge in some degree.

For bio-magnetic field detection in non-MSR at the room temperature, the circuit in-fan base noise level would better be less than 15mV (10pT resolution) at 1:5 signal to noise ratio. From the frequency perspective, the amplifier circuit should make signal above 200Hz attenuated, which can eliminate the high frequency electromagnetic disturbance. In addition, we also need to restrain power frequency disturbance using 50Hz and 100Hz notch filters. We need to design amplifier and filter circuit; whose gain is 10,000. And this circuit can filter out the frequency at 50Hz, 100Hz and above 200Hz. In addition, the in-fan base noise level needs to be less than 15mV.

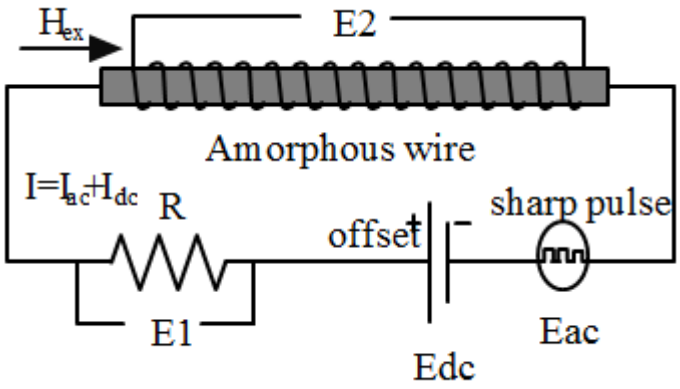

Fig. 3. Circuit diagram for off-diagonal GMI effect measurement. The external magnetic field change from -0.3ʒT to 3ʒT. Drive current *I* can be conquered by E1/R

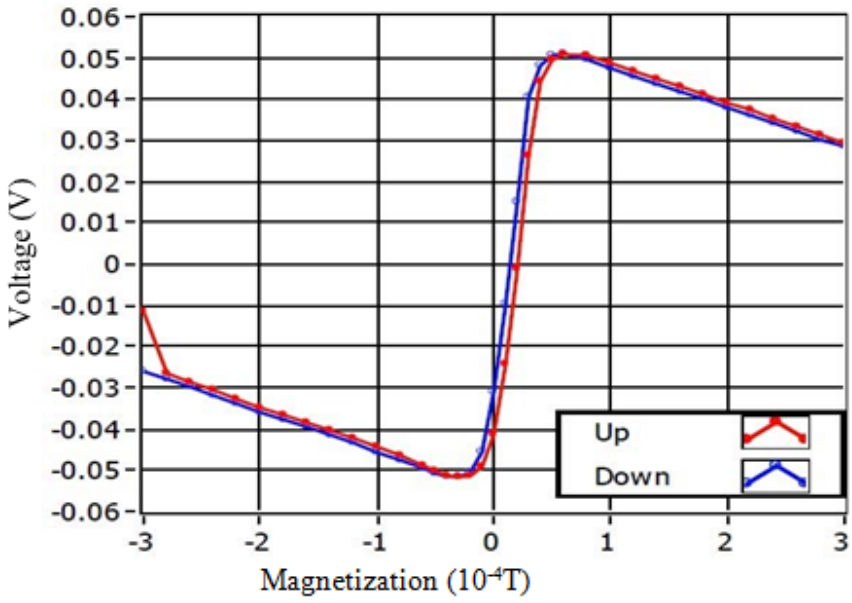

Fig. 4. The variation curves of off-diagonal GMI effect measurement.

V. CIRCUIT DESIGN

A. GMI head circuit:

The amorphous wire possesses poor consistency, i.e., different parts of amorphous wire own different optimum working point. To make amorphous wire work at the optimum working point, the sharp pulse current generator circuit we designed should be with easily adjustable pulse width and frequency.

Fig. 5 illustrates the sharp pulse generator circuit and GMI head circuit. The square-wave voltage generator (LTC 1799) produces a rectangular voltage train, ranging from 1kHz to 33MHz. The differential circuits transfer the square wave into

a positive sharp pulse. The current pulse train (2MHz) is applied to the amorphous wire as a carrier using Hex inverter (74AC04). A strong skin effect in amorphous wire will be caused due to a quick rising time around 100ns [1-9]. At the same time, the first pulse height of the induced voltage is proportional to the applied dc magnetic field. Hence, the Analog switch (SW:TS5A3166) should synchronously picks up the first pulse of induced voltage of two coils. [4].

B. Amplifier and filter circuit :

To obtain a stable and high gain (A>=100,000), the amplifier circuit is designed by several orders, because it is so difficult to obtain so much gain by only one order amplifier circuit. Beyond that we made use of the 200Hz high cut electric filters, 0.5Hz low cut electric filters (AC coupling, filter out DC component), 50Hz and 100Hz notch filters (eliminate power frequency interference) to prevent amplifier circuit saturation.

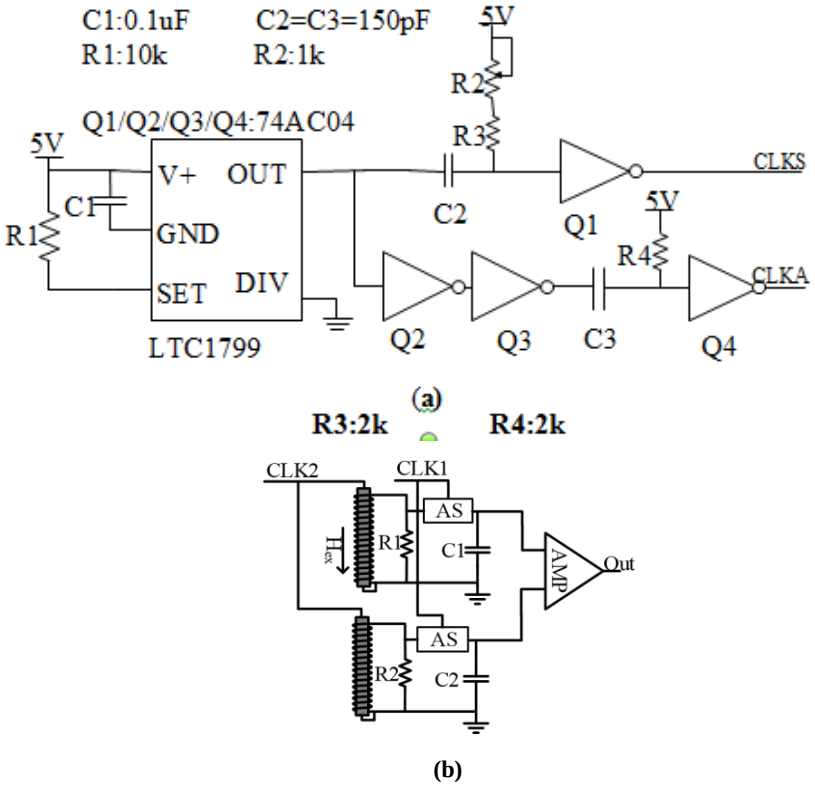

Fig. 5 Principle GMI sensor electronic circuit for bio-magnetic field detection. (a) Sharp pulse current generation circuit. (b) GMI head circuit

The circuit diagram for the gradiometer magnifying and filtering is shown in Fig. 6. The first part of Fig.6 illustrates the circuit of the pre-amplification circuit. Instrument amplifier IN128 was used in the first order. The INA128 is an integrated precision instrumentation amplifier offering high DC common mode rejection (CMR): 120dB min, and

low noise voltage: $10nV/Hz^{1/2}$. It should be noted that the gain of pre-amplification circuit cannot be set too large, or it would lead to sensor saturation. Besides, we applied autozero negative feedback to null the input offset voltage. The second part of Fig.6 shows the 50Hz notch filter circuit, we used twin T RC notch filter, the values of capacitance (C) and resistance (R) satisfy equations:C4=C5=C3/2, R3=R4=2R6, respectively. Here, we adopted precise resistance and capacitance to acquire exact 50Hz or 100Hz centre frequency. Before the notch filter circuit, we designed an AC coupled circuit (0.5Hz high-pass filter) to eliminate DC component with the purpose of preventing next-order circuit saturation. The gain can be set by R7 and R8 and not more than 100 times. In the third part of Fig. 6, we present two-order low-pass filter with 200Hz cut-off frequency. Same as above, we utilized AC coupled circuit to block DC component before low-pass filter. Generally, power frequency disturbance (50Hz in frequency, several nT in magnetic intensity), which could lead to bio-sensor saturation, includes not only 50Hz but also the second (100Hz) and third harmonic (150Hz) component. In the detection of human bio-magnetic field, the 50Hz fundamental component and 100Hz harmonic component have the largest impact on sensor performance. Hence, it is essential to eliminate the 100Hz disturbance. So, we add 100Hz twin T notch filter in the last order.

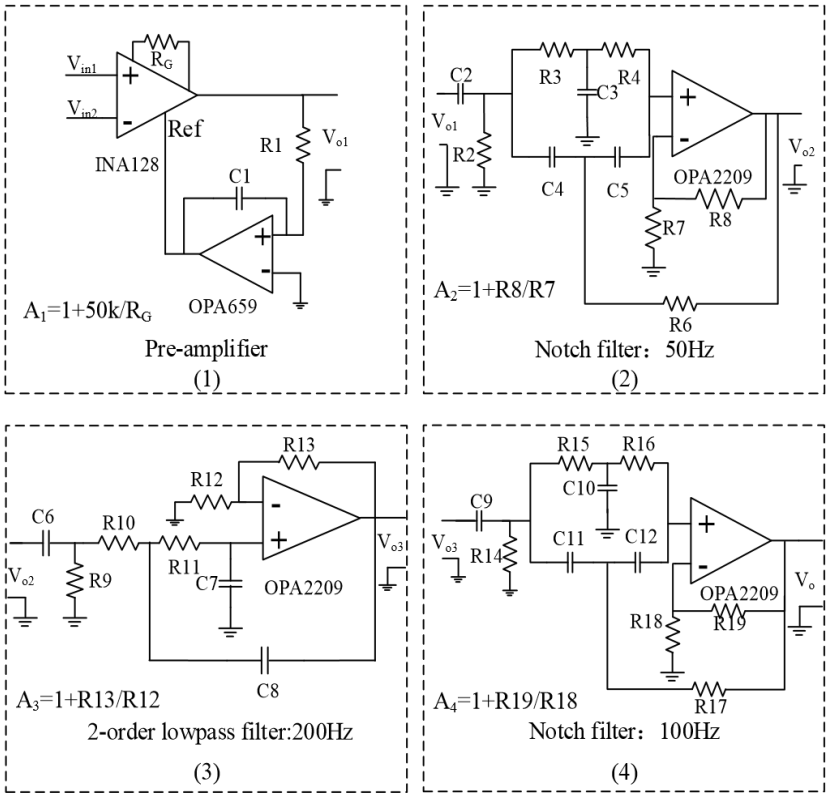

Fig. 6. Circuit diagram of the magnifying and filtering circuit for bio-magnetic field detection. The total gain: A=A1·A2·A3·A4, and A1~A4 are all no more than 100 times

VI. PERFORMANCE TESTING

Before circuit performance testing, we electrified the new circuit for half-hour to let the whole system work stably. We first test amplifier and filter circuit to conquer magnification. We use signal generator (RIGOL DG4162) to output sine wave (20Hz in frequency and 20mV in amplitude). By connecting V_{in1} to V_{in2}, we measured output V_{o2} to get the gain of the pre-amplifier and the secondary amplifier. We conquered the gain of remaining circuit using the same way stated above. Per the test result, the amplification reaches to 100 thousand. This circuit gain was set in 40 thousand times in the following test. Then we carried out circuit noise level testing. The test method was shorting V_{in1} and V_{in2}, and observed the output V_o by oscilloscope (Agilent DSO7012B). Fig. 7 shows the test result analysed in laptop, it is obvious that the main component of in-fan base noise level is less than 10mV.

In the following test, we carried out the noise test of whole bio-magnetic sensor. We connected C1, C2

(illustrates by Fig.5) to $V_{in1,}$ V_{in2}, respectively. The test environment was in the centre of a $120m^2$ assembly room without magnetic shielding. Fig. 8 illustrates the test result; we can easily conclude that the main part of whole biosensor system noise is more than amplifier circuit.

Per Ampere circuital theorem, the straight electric conducting wire will generate circular magnetic field, calculated by (7) as follows:

$$B = \frac{\mu_0 I}{2\pi r} \qquad (7)$$

where u_0 is magnetic permeability of vacuum (u_0= 4π×

$10^{-7}T{\cdot}m/A$), I is current and r is diameter. If we electrify a long enough straight wire with sinusoidal current, it will generate sinusoidal circular magnetic field. We can use this method for sensitivity detection of the bio-magnetic sensor.

Fig. 9 illustrates the time-domain waveform and frequency domain characteristics of output voltage. We used 50pT sinusoidal magnetic field for the sensitivity test. From the output waveform, we can observe the curve of sine wave. If we use the frequency-domain information, the sensitivity of the bio-magnetic sensor will improve a lot.

VII. CONCLUSION AND DISCUSSION

Based on the pulse giant Magneto-Impedance effect in Co-rich amorphous wire, we designed a sensor circuit for bio-magnetic field detection, including pulse generation circuit, GMI head circuit and amplifier circuit. To satisfy the special requirement for the detection of bio-magnetic field, we merely kept low frequency component, namely below 200Hz. Besides the power frequency interference at non-MRS reaches nT level. So, we made use of 50Hz and 100Hz notch filter to eliminate power magnetic interference, plus doing so also can prevent sensor saturation. We make the circuit into an Analog circuit board and preliminary test the circuit performance. In the performance test, we applied low current to a long enough straight wire to generate 50pT sinusoidal circular magnetic field and utilizing oscilloscope to observe the sensor output voltage, from the Fig.9, it is easily concluded that the sensitivity in time-domain might be more than 50pT. If we use the frequency-domain to analyse the sensitivity of bio-magnetic sensor, the sensitivity may improve a lot.

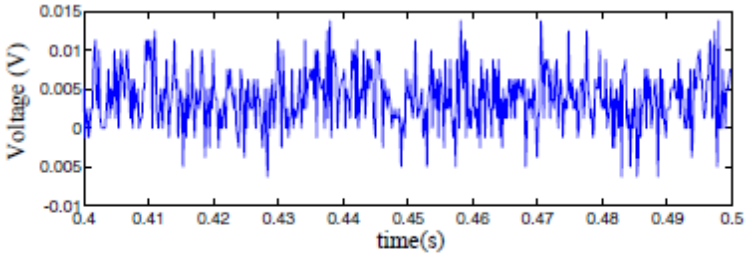

Fig.7 The in-fan base noise of the magnifying and filtering circuit. The base noise level is less than 15mV.

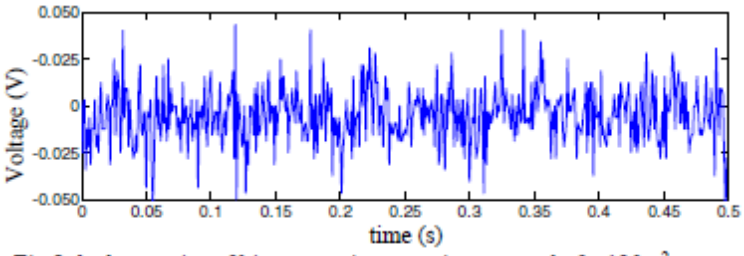

Fig.8 the base noise of bio-magnetic sensor in at central of a 120m^2 room without magnetic shielding. It is noted that the main part of sensor noise is less than 30mV.

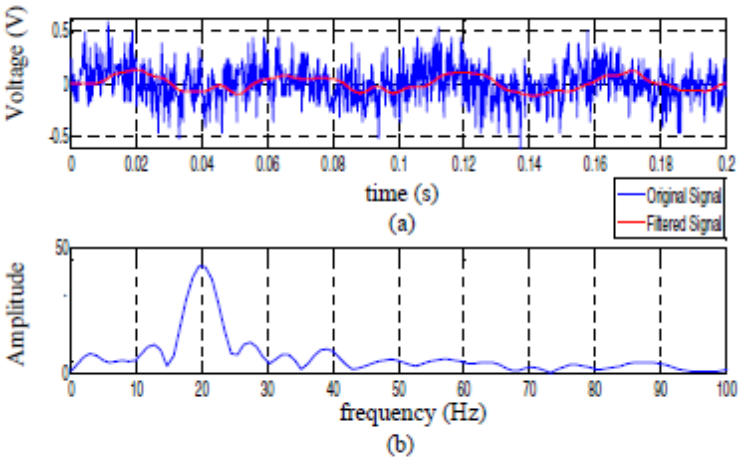

Fig. 9 Time-domain waveform and frequency spectrum of output signal filtered by yulewalk filter. The magnetic intensity is 50pT, and the frequency is 20Hz. (a) time-domain waveform (b) frequency spectrum.

If we manufacture the bio-sensor by MEMS and CMOS technology, the circuit performance could improve a lot.

ACKNOWLEDGMENT

I am grateful to Prof: D. K. Nayak (Principle) and Prof: Walavalkar (HOD of Humanities Dept.) of VPM`s Polytechnic for inspiring me for this effort. I am also grateful to Mrs. Raji Nair (Physics Lecturer) to assist with Circuit Designing of Bio-Magnetic Sensor Using Giant Magneto-Impedance Effect.

REFERENCES

[1] K. Mohri and Y. Honkura, "Amorphous wire and CMOS IC based magneto-impedance sensors—origin, topics, and future," *Sensor Letters*, vol. 5, no. 1, pp. 267–270, 2007.

[2] T. Uchiyama, K. Mohri, Y. Honkura, and L. V. Panina, "Recent Advances of Pico-Tesla Resolution Magneto-Impedance Sensor Based on Amorphous Wire CMOS IC MI Sensor," *IEEE TRANSACTIONS ON MAGNETICS*, vol. 48, no. 11, November 2012.

[3] K. Mohri, T. Uchiyama, L. Panina, "Recent Advances of Amorphous Wire CMOS IC Magneto-Impedance Sensors: Innovative HighPerformance Micro-magnetic Sensor Chip," *Journal of Sensors*, vol. 2015, No 718069, June 2015.

[4] K. Mohri and Y. Honkura, "Amorphous wire and CMOS IC based magneto-impedance sensors—origin, topics, and future," *Sensor Letters*, vol. 5, no. 1, pp. 267–270, 2007.

[5] T. Uchiyama, K. Mohri, Y. Honkura, and L. V. Panina, "Recent Advances of Pico-Tesla Resolution Magneto-Impedance Sensor Based on Amorphous Wire CMOS IC MI Sensor," *IEEE TRANSACTIONS ON MAGNETICS*, vol. 48, no. 11, November 2012.

[6] K. Mohri, T. Uchiyama, L. Panina, "Recent Advances of Amorphous Wire CMOS IC Magneto-Impedance Sensors: Innovative HighPerformance Micro-magnetic Sensor Chip," *Journal of Sensors*, vol. 2015, No 718069, June 2015.

[7] Tsuyoshi Uchiyama, Shinsuke Nakayama, "Magnetic sensors using amorphous metal materials: detection of premature ventricular magnetic waves," *Physiological Reports*, ISSN 2051-817X, June 2013.

[8] T. Uchiyama, K. Mohri, and S. Nakayama, "Measurement of spontaneous oscillatory magnetic field of guinea-pig smooth muscle preparation using pico-tesla resolution amorphous wire magnetoimpedance sensor," *IEEE Transactions on Magnetics*, vol. 47, no. 10, pp. 3070–3073, 2011.

[9] K. Mohri, Y. Honkura, L. V. Panina, and T. Uchiyama, "Super MI sensor: recent advances of amorphous wire and CMOS IC magnetoimpedance sensor," *Journal of Nanoscience and Nanotechnology*, vol. 12, no. 9, pp. 7491–7495, 2012.

[10] Nakayama, S., S. Atsuta, T. Shinmi, and T. Uchiyama, "Pulse-driven magnetoimpedance sensor detection of Bio-magnetic fields in musculatures with spontaneous electric activity," *Biosens. Bioelectron*, vol. 27, pp.34–39. 2011a.

[11] P. Ripka and L. Kraus, "Magnetoimpedance and magneto- inductance," in Magnetic Sensors and Magnetometers, P. Ripka, Ed. Norwood, MA: Artech House, pp. 350-358 , 2001

[12] Yoshinobu Honkura, "Development of amorphous wire type MI sensors for automobile use," *Journal of Magnetism and Magnetic Materials*, vol. 249, pp. 375–381, 2002.

[13] H. Hauser, R. Steindl, C. Hausleitner, A. Pohl, and J. Nicolics, "Wirelessly interrogable magnetic field sensor utilizing giant magneto-impedance effect and surface acoustic wave devices," *IEEE Trans. Instrum. Meas.*, vol. 49, pp. 648-652, 2000.

[14] L. G. C. Melo, D. Menard, A. Yelon, L. Ding, S. Saez, and C. Dolabdjian, "Optimization of the magnetic noise and sensitivity of giant magnetoimpedance sensors," *J. Appl. Phys*. vol. 103, pp. 033903-1-03303-6, 2008.

[15] T. Uchiyama, S. Nakayama, K. Mohri, and K. Bushida, "Biomagnetic field detection using very high sensitivity magneto-impedance sensors for medical applications," *Phys. Status Solidi A 206*, no. 4, pp. 639– 643, 2009.

[16] H. Chiriac, M. Tibu, V. Dobrea, and I. Murguleacu, "Thin Amorphous Wires for GMI Sensor," *Journal of Optoelectronics and AdvancedMaterials*, vol. 2, no. 2, pp. 647–650, 2004.

[17] S. Sandacci, D. Makhnovskiy, L. Panina, K. Mohri, and Y. Honkura, "Off-diagonal impedance in amorphous wires and its application to linear magnetic sensors," *IEEE Trans. Magn.*, vol. 40, no. 6, pp. 18– 23, 2008.

[18] J.F. Hu, H.W. Qin, F.Z. Zhang, R.K. Zheng, *J. Appl. Phys.* 91 (2002) 7418–7420.

[19] C. J. Harland, T. D. Clark, and R. J. Prance, "Remote detection of human electroencephalograms using ultrahigh input impedance electricpotential sensors," *Appl. Phys. Lett.*, vol. 81, no. 17, 3284, (2002).